DOI: 10.21062/mft.2023.017 http://www.journalmt.com

Use of Electron Microscopy in the Analysis of the Influence of Roughness on the Corrosion Behavior of Selected Ti Alloys

Iryna Hren (0000-0003-3942-2481), Sylvia Kuśmierczak (0000-0002-5135-4170), Roman Horký (0000-0002-4451-3006)
Faculty of Mechanical Engineering, J. E. Purkyne University in Usti nad Labem. Pasteurova 3334/7, 400 01 Usti nad Labem. Czech Republic. E-mail: sylvia.kusmierczak@ujep.cz, iryna.hren@ujep.cz

Titanium alloys are among the biocompatible materials that are used for biomedical implants. From the point of view of the reactivity of the human body, it is important to know the state of the surface of these materials, which in technical practice is represented by the term surface integrity, which includes a complex of evaluated properties. One of the classic approaches is the evaluation of the surface roughness and the properties of the stable oxide layer, which influence the formation of the connection of the implant with human tissues and influence its acceptance. Another frequent approach is the use of optical metallography, especially for the assessment of material thickness, distribution and character of corrosion attack. Less common is the use of electron microscopy in the evaluation of the surface, which in this case is affected by the action of corrosion. Samples of both pure titanium and Ti6Al4V alloy were divided into sets according to surface roughness and subsequently exposed to corrosion for different periods of time. The presented article is devoted to basic analyzes of the effect of roughness on corrosion behavior using not only classical optical but also electron microscopy.

Keywords: surface, titanium, corrosion, Ti6Al4V alloy, microscopy.

1 Introduction

Titanium as an element was discovered in 1791 by the English chemist William Gregor as part of the mineral ilmenite. After the Second World War, titanium-based alloys began to gain traction in industry, especially for the production of aircraft engine parts. Today, the use of titanium and its alloys is extended to most branches of industry [1,6,8,16]. Compared to other metals, titanium has certain unique properties: high corrosion resistance, significant mechanical properties and thermal load capacity, the highest ratio between strength and density of all metal materials, high tensile strength, high biocompatibility [7-8].

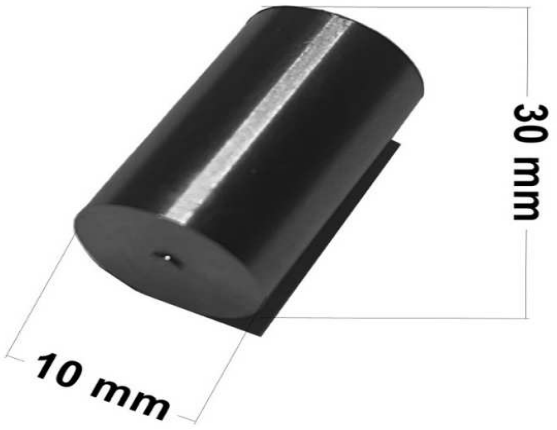

Fig. 1 *Sample cuttings off from the titanium rod*

Titanium alloys offer attractive properties such as high strength to weight ratio, high fracture resistance, good formability and biocompatibility. Thanks to these advantages, titanium alloys have found various technological applications in the marine, automotive, aeronautical and space industries. Titanium and its alloy have a high resistance to corrosion due to a compact and chemically stable oxide film that spontaneously forms on the surface of the metal. However, under certain harsh conditions, the anti-corrosion behaviour is also expected to improve [9-12]. Titanium and its alloys are, of course, the most used material in medicine, when using implants in the human body. In addition to all the mentioned advantages, another reason for using titanium and its alloys is that unlike nickel, which is a mandatory component of stainless steels, titanium does not cause allergic reactions in the human body [13 - 17].

Recently, however, there have been cases where corrosion has started to appear at the implants. Ti-6Al-4V alloy is a commonly used biomaterial in the biomedical implant industry, especially as a ball joint and oral implant (hip stems, screws and nuts), but it can suffer from friction and/or galvanic corrosion leading to material failure [18-22]. There is also growing concern about surface degradation of bio-implants in various corrosive environments. Dissolution of implant materials can cause an inflammatory reaction with internal organs and can be fatal [23-24].

The authors Bodunrin and Gudić in their works [25, 26] investigated whether the environment of salt fog or physiological solution has any effect on the corrosion of titanium. During the experiment, the temperatures in these environments were set to temperatures similar to the human body. The roughness of the titanium surface is also important in the human body. And this is mainly due to the fact that titanium belongs to the group of bioinert materials [27-28]. This means that it is fully acceptable for biological tissue, and it is possible to use different roughness's for titanium and its alloys, since the attachment of cells and tissues to the surface of the implant changes with different roughness's [29]. However, both pure titanium and the Ti-6Al-4V alloy have certain disadvantages, such as low shear strength and low wear resistance when used in orthopedic surgery. The discrepancy in Young's modulus between the titanium implant (100–120 GPa) and the bone (10–30 GPa) is also a problem, which is unfavourable for bone healing and remodelling [30-31].

On the other hand, its biocompatibility, low toxicity, high mechanical strength and low density make titanium an excellent material for the production of orthodontic, prosthetic and cardiovascular implants. Each such implant must last a lifetime in the human body, without the possibility of inspection and maintenance, and therefore their corrosion resistance is a priority. The most common solution used to study the electrochemical behaviour of a metal is to simulate a body fluid at pH 7.4. In specific cases, such as inflammation or orthodontic implants in the presence of toothpaste, the composition and pH may vary [32-33]. The roughness of titanium and its alloys is of great importance especially in the medical sector, especially when using titanium implants. With the help of research, it was found that thanks to the greater roughness of the titanium alloy, the creation and formation of new tissues is accelerated and improved. Also, due to the rougher surface, better attachment of cells, their faster growth and maturation was found.

2 Material and experiment

For the experiment, 2 types of materials were used. One was commercially pure titanium and the other is Ti-6Al-4V alloy. Titanium, in the form of pure titanium and the Ti-6Al-4V alloy, is used in medicine as an implant for bone tissue in orthopedics, neurosurgery, dentistry or in facial and plastic surgery. Currently, titanium is preferred especially for its physico-chemical properties, mechanical strength and good corrosion resistance. Titanium is increasingly used in devices that work in contact with seawater for a long time. The chemical composition of both alloys is shown in tab. 1 and 2.

Tab. 1 *Chemical composition of commercially pure titanium according to EN 10 204 3.1*

Commercially pure titanium								
O	**N**	**C**	**H**	**Fe**	**Al**	**V**	**Ni**	**Ti**
0.25	**0.03**	**0.08**	**0.015**	**0.3**	**-**	**-**	**-**	**99.25**

Tab. 2 *Chemical composition of Ti-6Al-4V alloy according to EN 10 204 3.1*

Titanium alloy with 6Al-4V elements								
O	**N**	**C**	**H**	**Fe**	**Al**	**V**	**Ni**	**Ti**
0.2	**0.05**	**0.08**	**0.015**	**0.4**	**5.8**	**3.7**	**-**	**90.12**

Both types of delivered material were prepared and delivered in the form of rods. The material was machined to the required roughness (Ra 3.2, Ra 1.7 and Ra 0.3) complete with equipment and conditions under which it was machined and subsequently cut into rolls of the same size: length – 30 mm and diameter – 10 mm (fig. .2).

Fig. 2 *Prepared rolls*

The next step of the experiment was the corrosion load of all samples carried out in a corrosion diagnostic device (corrosion chamber) LIEBISCH®. The working conditions of the salt chamber are governed by the ČSN EN ISO 9227 standard [30]. Specifically, it was a corrosion load for 168, 240, 480 and 720 hours. Then the samples were taken out of the salt chamber and cleaned of corrosion products. The samples were subsequently metallographically prepared: grinding, polishing, etching.

For the analysis of the microstructure of the layer and the base material, 24 samples were metallographically prepared - by wet grinding using sandpaper with a grain size of 120 to 2000 μm. Subsequently, polishing was carried out using the following emulsions from Struers: Al_2O_3 5 μm, diamond emulsion DIA 1 μm and Al_2O_3 0.3 μm. Grinding and polishing was performed on a SAPHIR 360 machine with a wheel speed of 300 and then 150 rpm-1. After subsequent etching of the mixtures with

a Kroll etchant, the material structures were observed using light microscopy on a LEXT OLS 5000 Olympus confocal laser microscope.

3 Microscopic evaluation without corrosion load

In the first stage, microscopic analysis of the alloy and commercially pure titanium samples was performed using an Olympus Lext 5000 laser microscope. Figure 3 characterizes the pure titanium samples without corrosion stress (denoted as C0), for which the α structure is typical. In this type of material, the main alloying element is aluminum Al, which stabilizes the α phase. Other elements and stabilizers (O, C, N) negatively affect the resulting mechanical properties and are therefore considered undesirable.

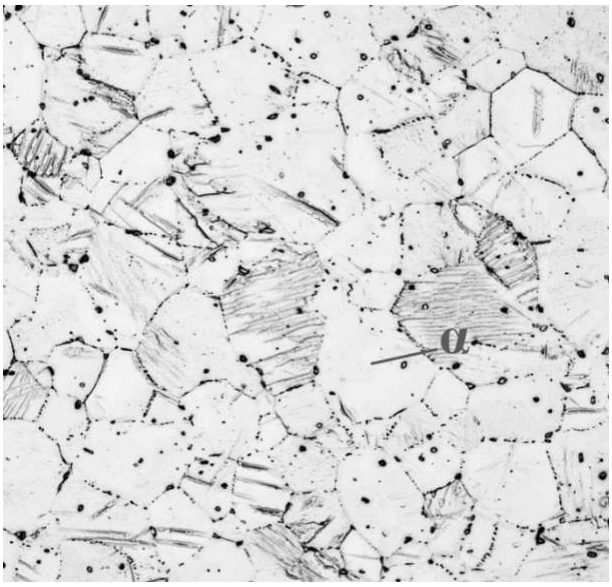

Fig. 3 *Microstructure of commercially pure titanium, sm. CO, mag. 200x*

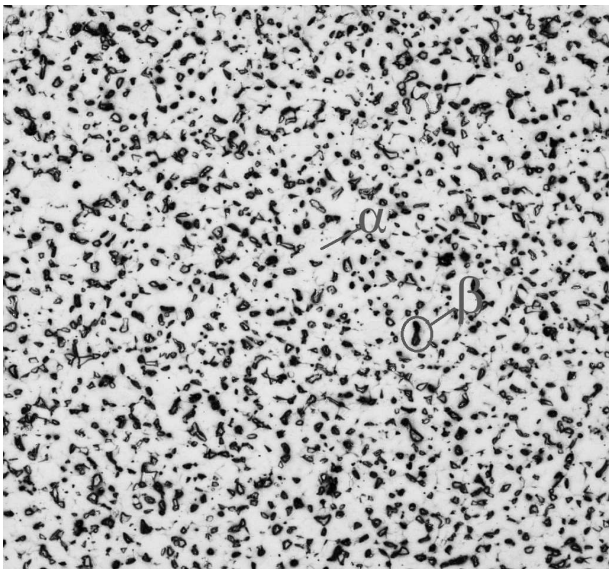

Fig. 4 *Microstructure of Ti-6Al-4V alloy, sm. S0, mag. 200x*

In contrast, the titanium alloy Ti-6Al-4V consists of α and β phases, see Fig. 4. These alloys belong to the category of so-called two-phase alloys. The structure is formed by phase β grains (dark grains). These phases are regularly and uniformly arranged around the α phase (light grains). The individual grains are distributed without the slightest clusters of one or the other phase. β-phase grains are smaller and irregular in shape compared to α-phase grains α-phase grains are larger and more regular in shape. As expected, the microstructure image of sample S0 showed a duplex microstructure containing α and β phases. These alloys contain a larger amount of aluminum (6 - 9 wt.% according to the wt.% of vanadium), which serves as a stabilizer of the α phase, and then a lower amount of alloying elements that serve as stabilizers of the β phase. The most important element for stabilizing the β phase is vanadium. Other alloys used in these alloys include Cr, Cu, Zr, which have the task of improving mechanical properties. In the case of some elements (especially heavy metals), there are concerns about their negative effects on the human organism, especially during long-term interaction with body fluids, especially in the case of joint replacements [34-37].

4 Microscopic evaluation of samples after corrosion loading

Evaluation of the TiO_2 corrosion layer in samples of commercially pure titanium and titanium alloy Ti-6Al-4V was carried out using a VEGA Tescan 3 electron microscope. Figures 5–8 document experimental samples of pure titanium that have been in a salt chamber for 168 hours. The experimental samples were divided according to the machining method. For samples unmachined and machined to a roughness parameter Ra of 0.3, 1.7 and 3.2.

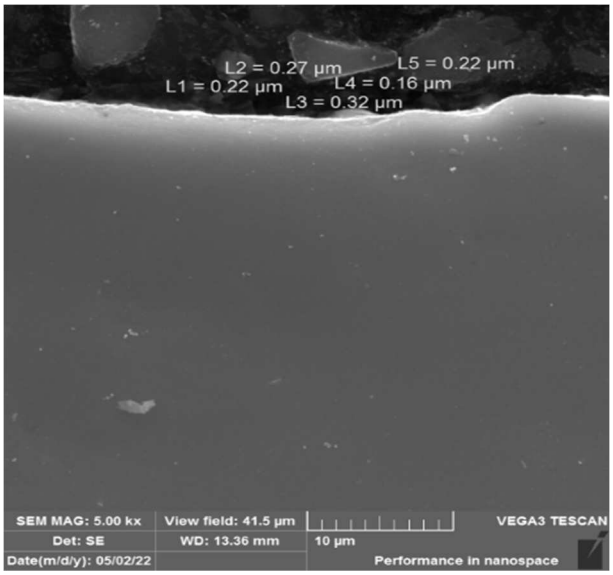

Fig. 5 *Condition of the surface layer, sample C1*

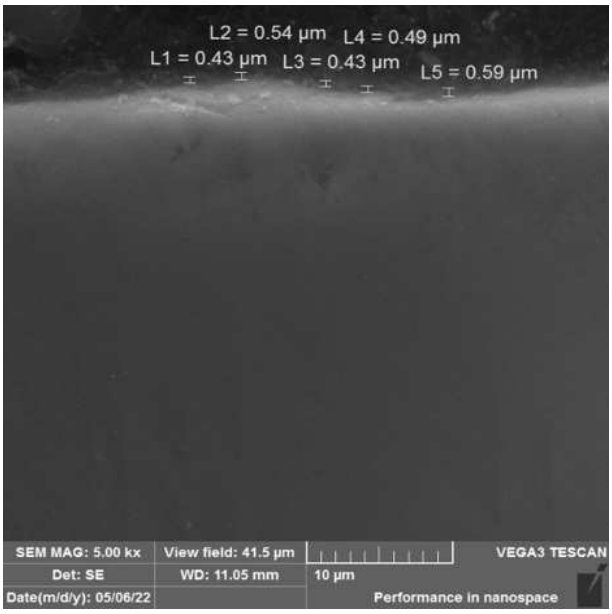

Fig. 6 *Condition of the surface layer, sample CR11*

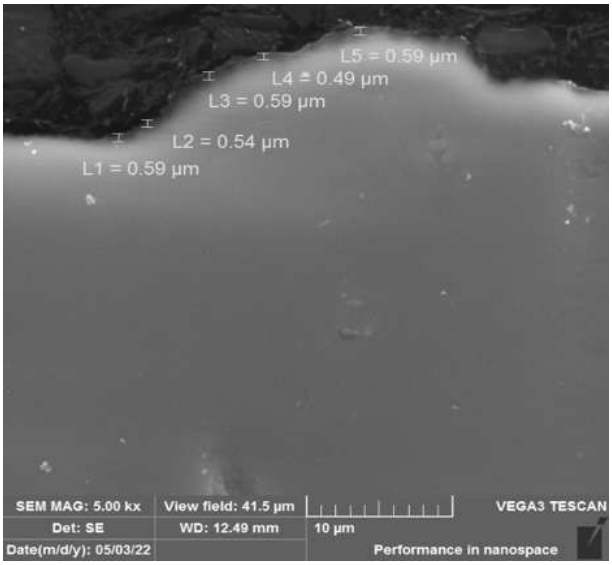

Fig. 7 *Condition of the surface layer, sample CR21*

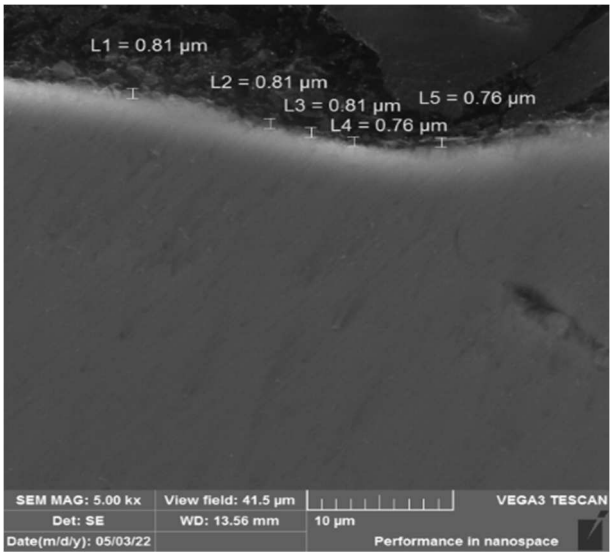

Fig. 8 *Condition of the surface layer, sample CR31*

A TiO_2 layer with an average thickness of 0.25 µm was observed for the first investigated sample, which was designated as C1. Another sample labeled as CR11 in Fig. 6 had an oxidation layer with an average thickness of 0.48 µm. Compared to the CR11 sample, the CR21 experimental sample had an increase in the thickness of the TiO_2 oxidation layer by 0.08 µm. The largest thickness of the TiO_2 oxidation layer on the surface of the examined material is observed in the sample labeled CR31, namely 0.79 µm, which was documented in Fig. 8. All experimental samples were in the salt chamber for 168 hours and it was observed that with increasing roughness, the average thickness of the TiO_2 oxidation layer on the surface also increases.

In the following sequence of Fig. 9–12, we can observe the microstructure of the samples and examine the TiO_2 oxidation layer. The experimental samples are divided according to the roughness parameter, under a corrosion load in a salt chamber for 240 hours.

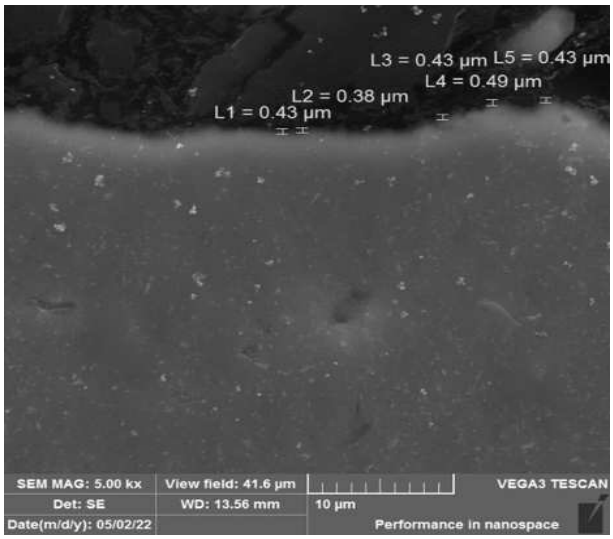

Fig. 9 *Condition of the surface layer, sample C2*

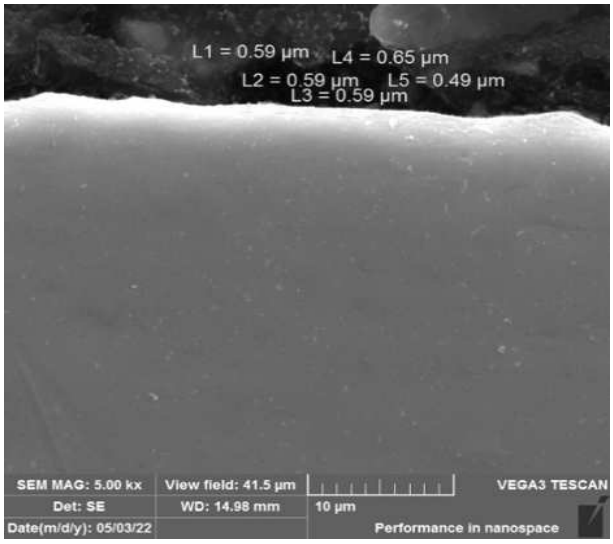

Fig. 10 *Condition of the surface layer, sample CR12*

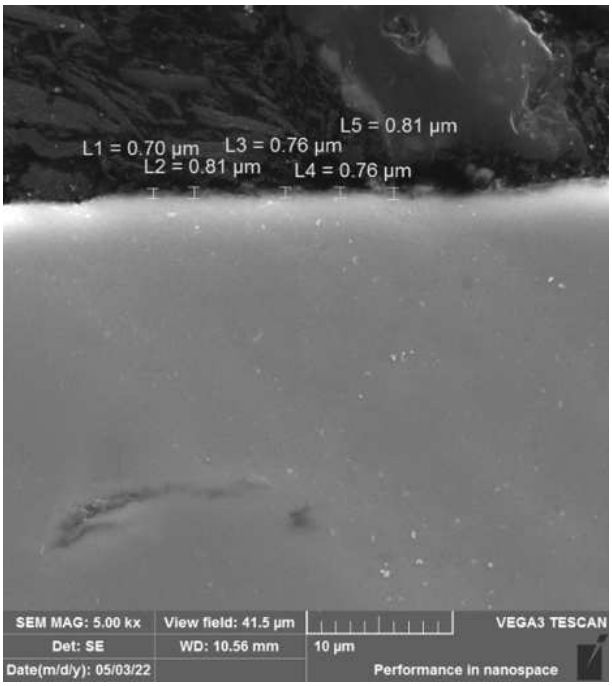

Fig. 11 *Condition of the surface layer, sample CR22*

For experimental samples loaded for 240 hours in a salt chamber, we can observe that the thickness of the TiO_2 oxidation layer increases with increasing roughness. The average thickness of the oxidation layer in the untreated sample C2 is 0.43 µm. The next sample measured was a sample machined to a roughness parameter of Ra 0.3 and has the designation CR12. For this sample, the thickness of the TiO_2 oxidation layer was measured to be 0.58 µm. For the experimental sample labeled CR22, the average thickness of the oxidation layer on the surface was measured to be 0.77 µm. The largest average thickness of the TiO_2 oxidation layer was measured for the CR32 sample, namely 0.85 µm.

For better clarity, the data obtained with the help of an electron microscope are shown in tab. 3.

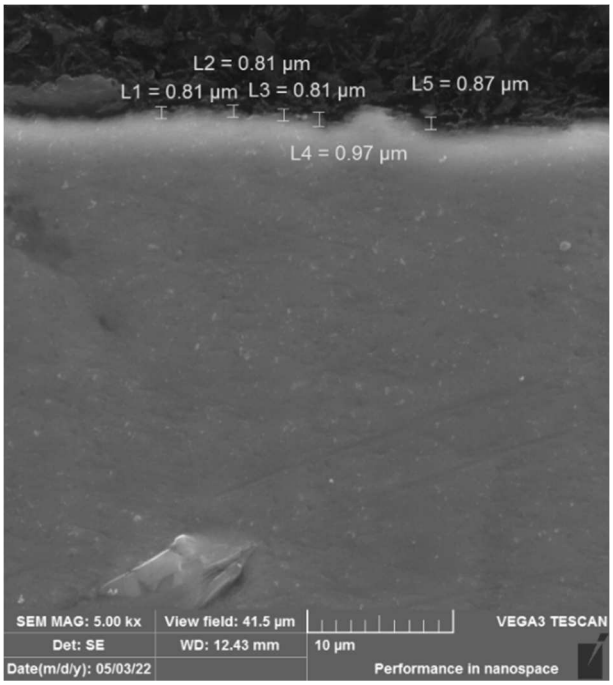

Fig. 12 *Condition of the surface layer, sample CR32*

Tab. 3 *Measured values of layer thickness*

	C1	CR11	CR21	CR31	C2	CR12	CR22	CR32
L1 [µm]	0.22	0.43	0.59	0.81	0.43	0.59	0.7	0.81
L2 [µm]	0.27	0.54	0.54	0.81	0.38	0.59	0.81	0.81
L3 [µm]	0.32	0.43	0.59	0.81	0.43	0.59	0.76	0.81
L4 [µm]	0.16	0.49	0.49	0.76	0.49	0.65	0.76	0.97
L5 [µm]	0.22	0.59	0.59	0.76	0.43	0.49	0.81	0.87
øL [µm]	0.238	0.496	0.56	0.79	0.432	0.582	0.768	0.854
stan. Dev. σ	0.0538	0.0625	0.0400	0.0245	0.0349	0.0515	0.0407	0.0625

The experimental samples, which were in the salt chamber for 480 hours, are divided according to the machining method to commercially pure titanium without any machining and machining to the roughness parameter Ra 0.3, 1.7 and 3.2, see Fig. 13–16.

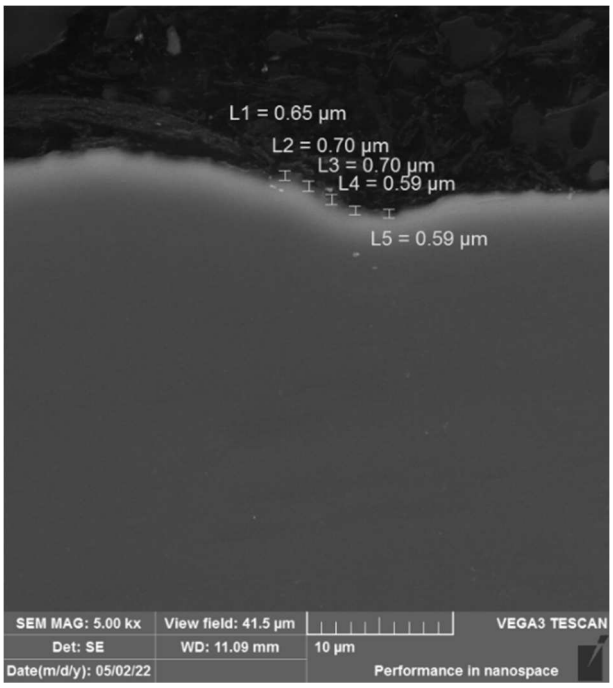

Fig. 13 *Condition of the surface layer, sample C3*

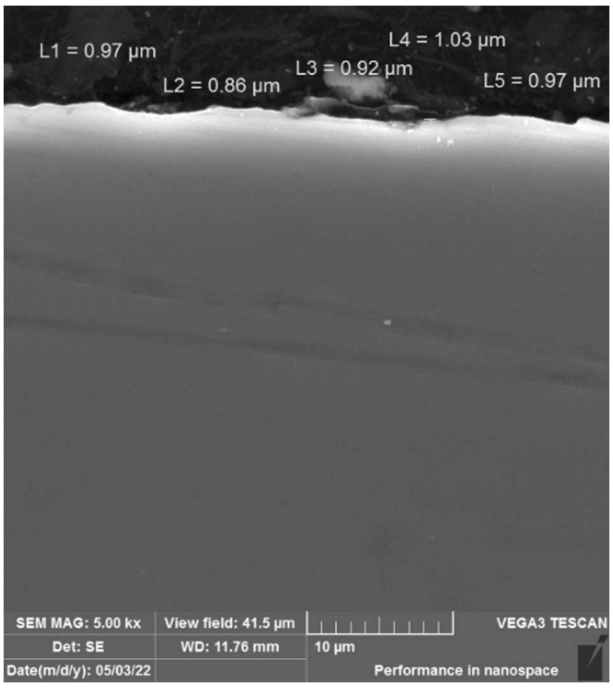

Fig. 14 *Condition of the surface layer, sample CR13*

The experimental samples, which were in the salt chamber for 480 hours, are divided according to the machining method to commercially pure titanium without any machining and machining to the roughness parameter Ra 0.3, 1.7 and 3.2, see Fig. 13–16. All experimental samples taken out of the salt chamber after 480 hours have a continuous and compact TiO_2 oxidation layer on the surface. We can observe that as the roughness increases, the thickness of the TiO_2 oxidation layer on the surface of the examined samples also increases. The first examined sample labeled C3 has an average thickness of the oxidation layer of 0.65 µm. For another experimental sample labeled CR13, the average thickness of the oxidation layer was measured to be 0.95 µm. The third experimental sample labeled CR23 has an average oxide layer thickness of 1.04 µm after measurement on the surface. The largest thickness of the TiO_2 oxidation layer was measured on the surface of the experimental sample CR33 and was 1.07 µm. Experimental samples of pure titanium, see Fig. 17–20, which were loaded in the corrosion environment of the salt chamber for 720 hours, are divided according to the roughness parameter.

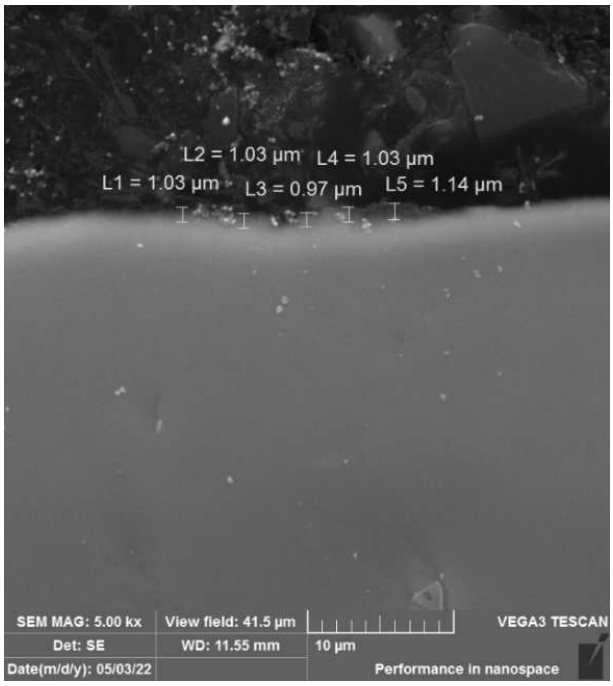

Fig. 15 *Condition of the surface layer, sample CR23*

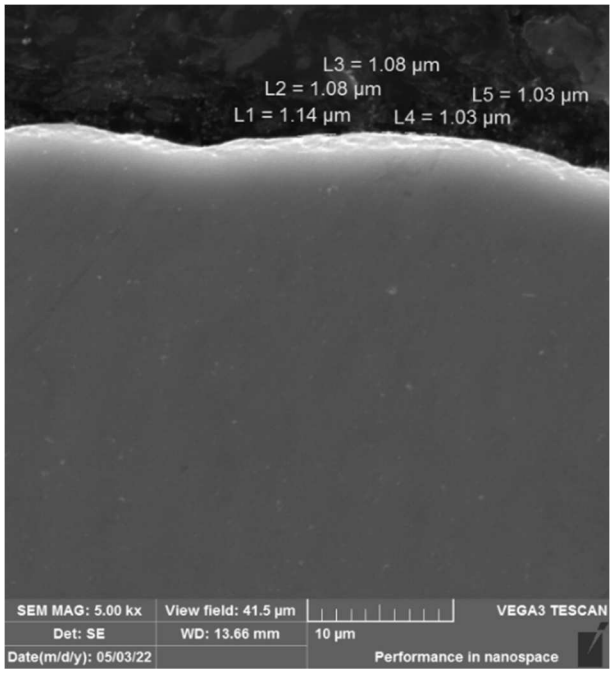

Fig. 16 *Condition of the surface layer, sample CR33*

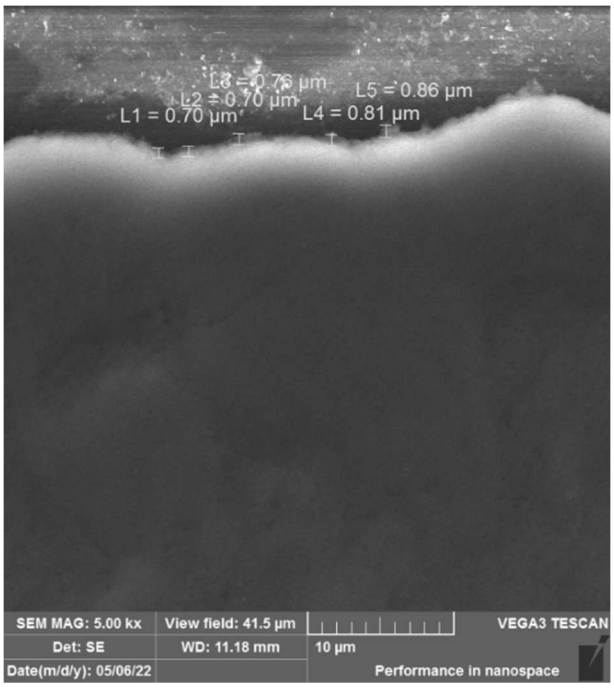

Fig. 17 *Condition of the surface layer, sample C4*

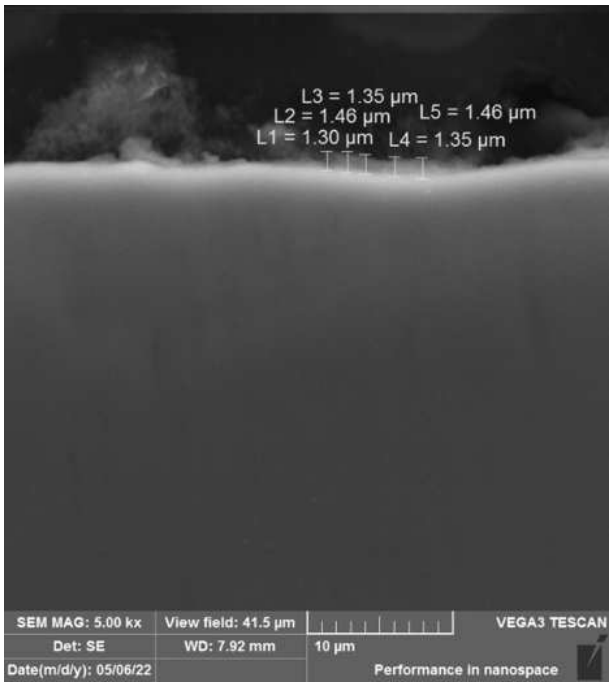

Fig. 19 *Condition of the surface layer, sample CR24*

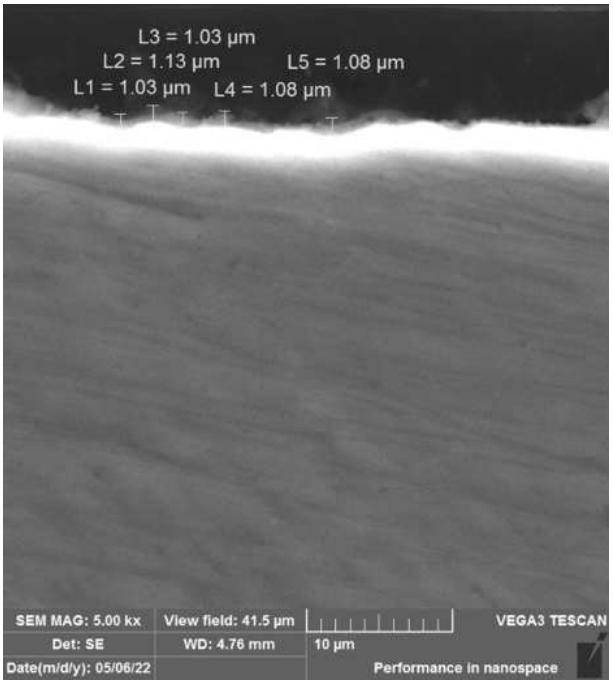

Fig. 18 *Condition of the surface layer, sample CR14*

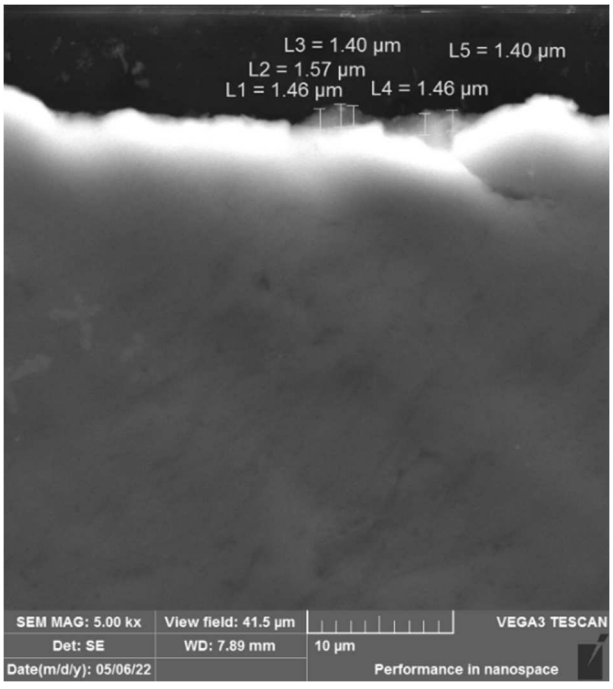

Fig. 20 *Condition of the surface layer, sample CR34*

Tab. 4 *Measured values of layer thickness*

	C3	CR13	CR23	CR33	C4	CR14	R24	CR34
L1 [µm]	0.65	0.97	1.03	1.14	0.7	1.03	1.3	1.46
L2 [µm]	0.7	0.86	1.03	1.08	0.7	1.13	1.46	1.57
L3 [µm]	0.7	0.92	0.97	1.08	0.76	1.03	1.35	1.4
L4 [µm]	0.59	1.03	1.03	1.03	0.81	1.08	1.35	1.4
L5 [µm]	0.59	0.97	1.14	1.03	0.86	1.08	1.46	1.46
øL [µm]	0.646	0.95	1.04	1.072	0.766	1.07	1.384	1.458
stan. Dev. σ	0.0492	0.0569	0.0551	0.0407	0.0625	0.0374	0.0647	0.0621

The first sample measured after corrosion loading for 720 hours was the sample labeled C4. An average TiO_2 oxidation layer with a thickness of 0.77 μm was measured on the surface of the sample. On the next observed sample labeled CR14, an average oxidation layer with a thickness of 1.07 μm was measured on the surface. An oxidation layer of 1.38 μm was measured for the sample labeled CR24. The largest TiO_2 oxidation layer on the titanium surface was measured for the CR34 sample with a roughness parameter Ra of 3.2. The average thickness of the oxidation layer of this experimental sample was 1.46 μm.

For better clarity, the data obtained with the help of an electron microscope are shown in tab. 4.

5 Ti-6Al-4V alloy in the corrosion environment of a salt chamber

Due to the detection and measurement of very small oxidation layers of TiO_2 on the surface of the Ti-6Al-4V alloy for all roughness parameters and times of corrosion action in the salt chamber, we do not evaluate the thickness of the oxidation layer, but the occurrence of titanium oxides on the surface of the examined material. The evaluation is carried out using a VEGA Tescan 3 electron microscope and subsequent EDS analysis and mapping. Na and Cl particles were filtered out from EDS analysis and mapping in order to prevent visual contamination during mapping and analysis using EDS analysis. The same surface condition was observed for samples subjected to corrosion loading in a salt chamber for 240 hours as for 168 hours corrosion loading.

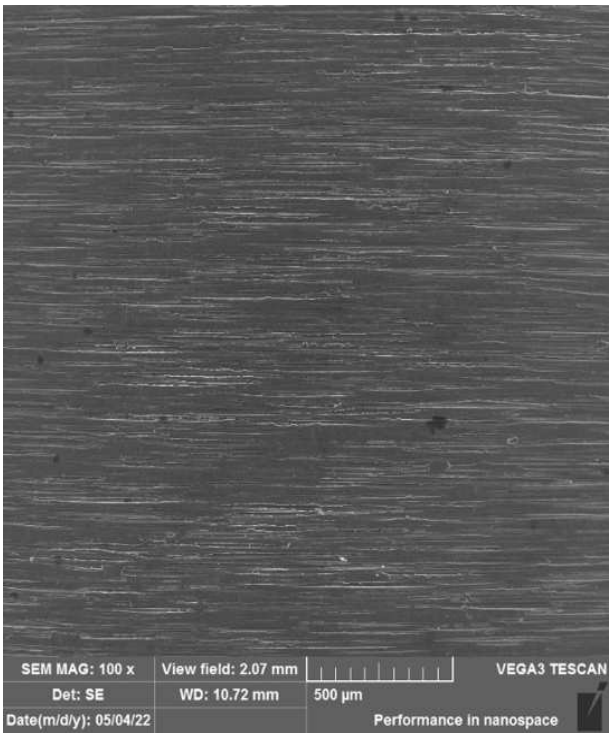

Fig. 21 *Surface condition of the sample S1*

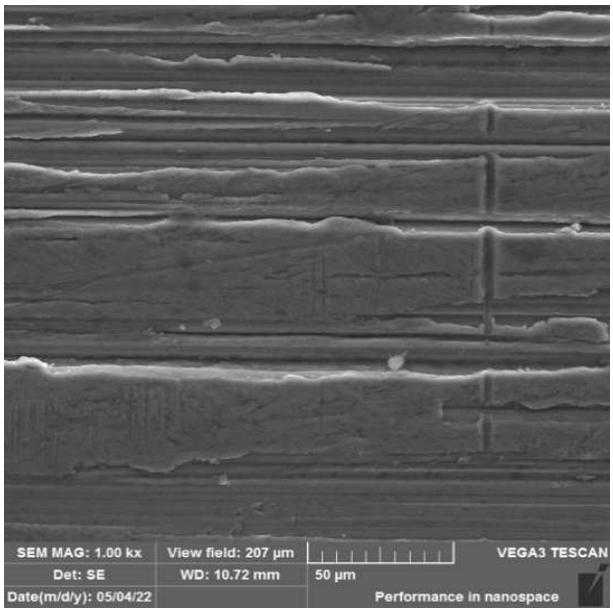

Fig. 22 *Surface condition of the sample S1, detail*

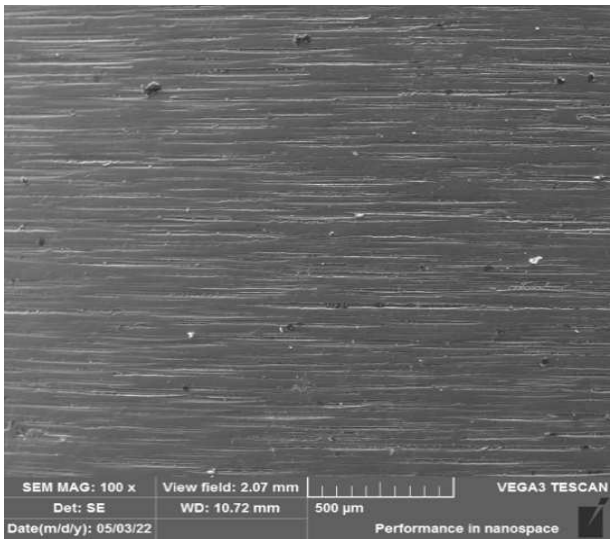

Fig. 23 *Surface condition of the sample S2*

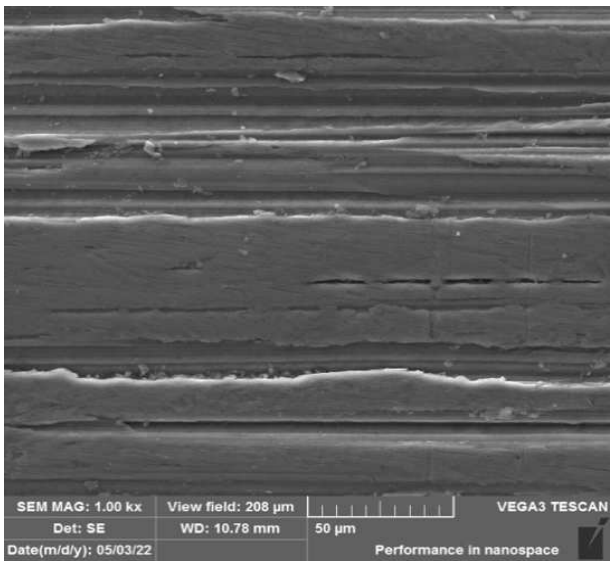

Fig. 24 *Surface condition of the sample S2, detail*

For this reason, images documenting these surfaces are not presented in the work. In Fig. 21–24, samples S1 and S2 were documented, for which surface observation was performed, then EDS analysis was performed, but no occurrences of oxide appeared on the surface of the examined samples at 168 and 240 hours in the salt chamber. For this reason, surface mapping was no longer carried out.

In the case of experimental sample S3, it can be seen that thanks to EDS analysis and subsequent mapping, it was possible to document that oxides (O = 3.68 wt.%) occur on the surface of the examined material (Fig. 25), which is also confirmed by mapping and surface EDS analysis (Fig. 26). This analysis confirmed that the oxides are evenly distributed on the surface.

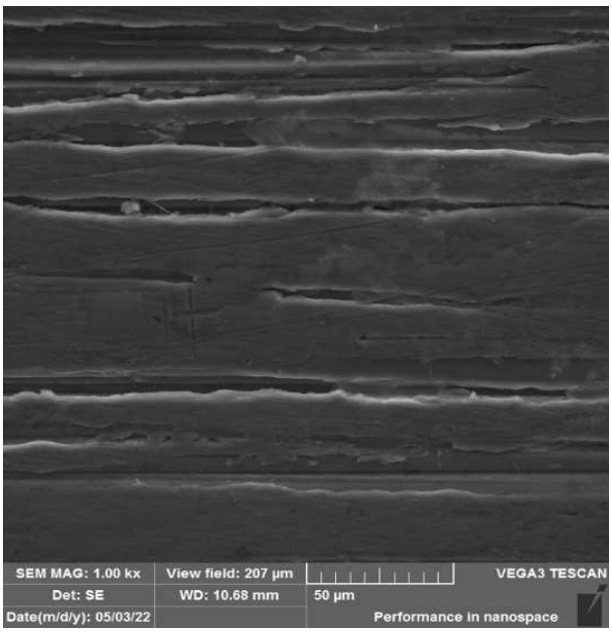

Fig. 25 *Surface condition of the sample S3, detail*

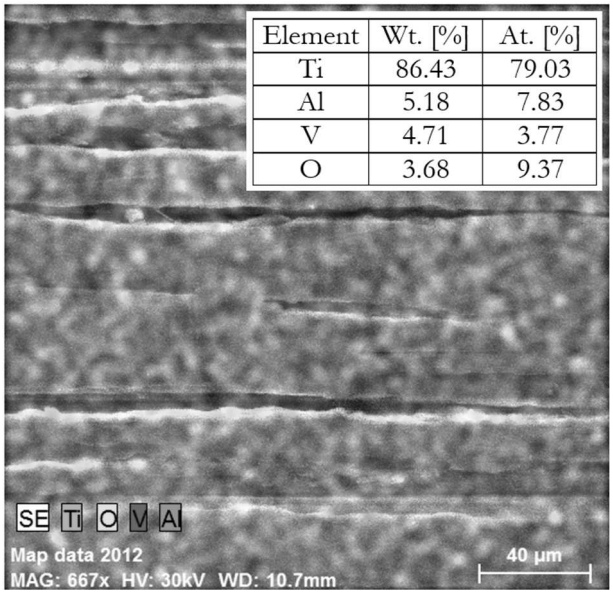

Fig. 26 *Result of EDS analysis and surface mapping*

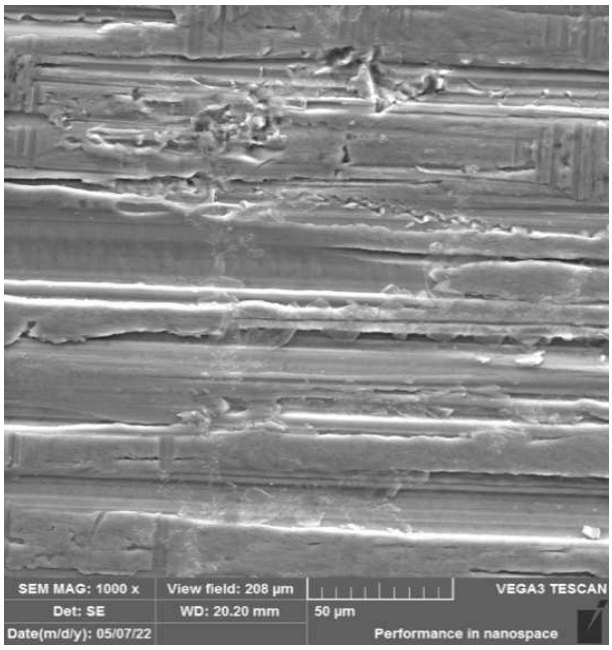

Fig. 27 *Surface condition of sample S4, detail*

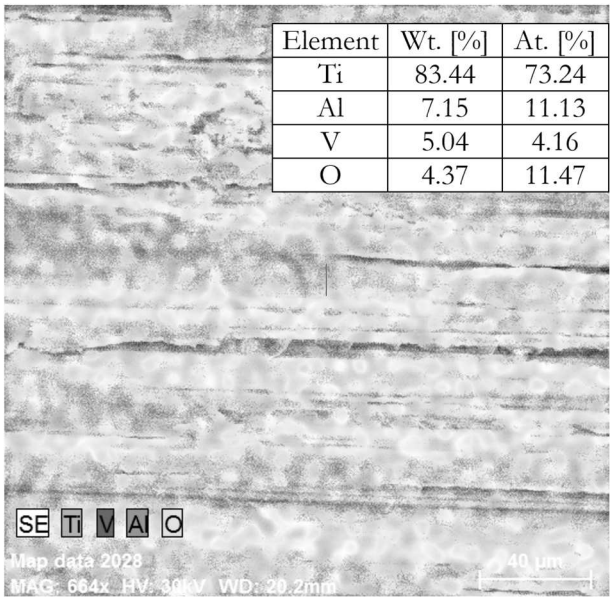

Fig. 28 *Result of EDS analysis and surface mapping*

For the observed sample labeled S4 (Fig. 27), which was in the salt chamber for 720 hours and was not processed in any way, it was confirmed by EDS analysis that there is oxide in a slightly larger amount on the surface of the examined material than in the previous sample (O = 4.37 wt.%). Thanks to the use of surface EDS analysis and subsequent mapping, it was found that the oxide spreads evenly over the entire surface of the observed experimental sample (Fig. 28). The next images (Fig. 29) document the microstructure of the surface of the SR11 sample, which had a roughness parameter Ra of 0.3 and was subjected to corrosion loading in a salt chamber for 168 hours. No oxide formation was found on the surface of the experimental sample (Fig. 30, O = 0.00 wt. %).

ISSN 1213–2489
e-ISSN 2787–9402

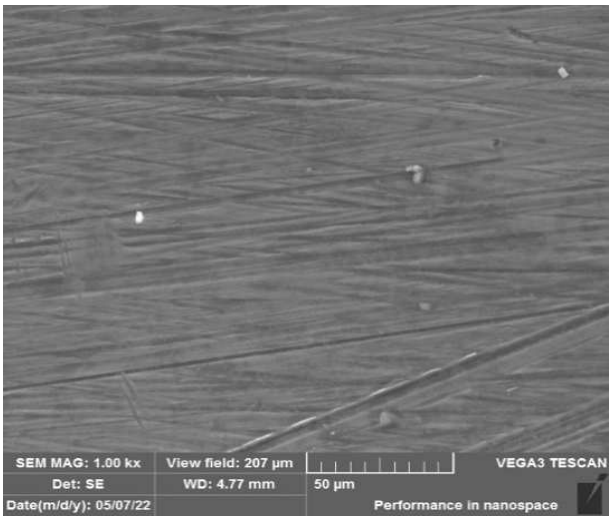

Fig. 29 *Surface condition of sample SR11, detail*

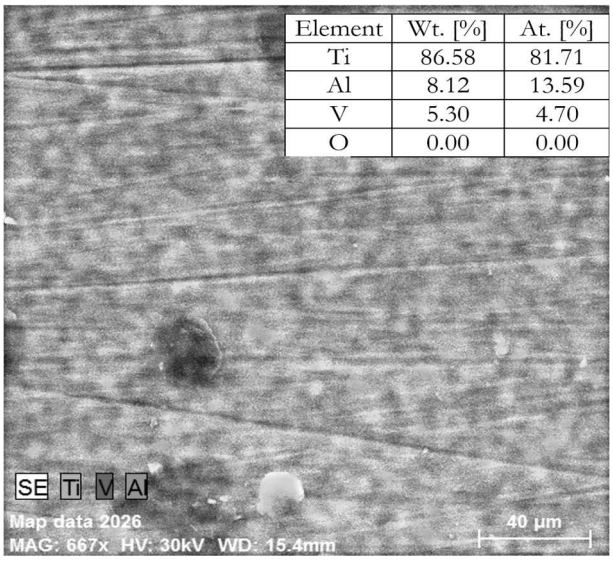

Element	Wt. [%]	At. [%]
Ti	86.58	81.71
Al	8.12	13.59
V	5.30	4.70
O	0.00	0.00

Fig. 30 *Result of EDS analysis and surface mapping*

The following SR21 sample, which was subjected to corrosion attack in a salt chamber for 168 hours with a roughness parameter Ra of 1.7, and its microstructure is shown in Fig. 31.

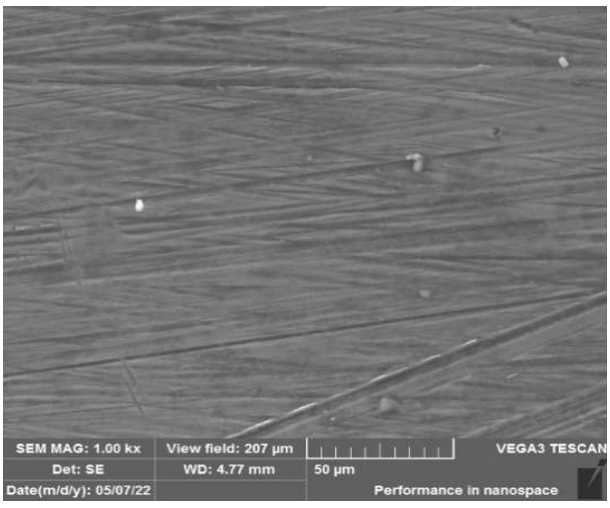

Fig. 31 *Surface condition of sample SR21, detail*

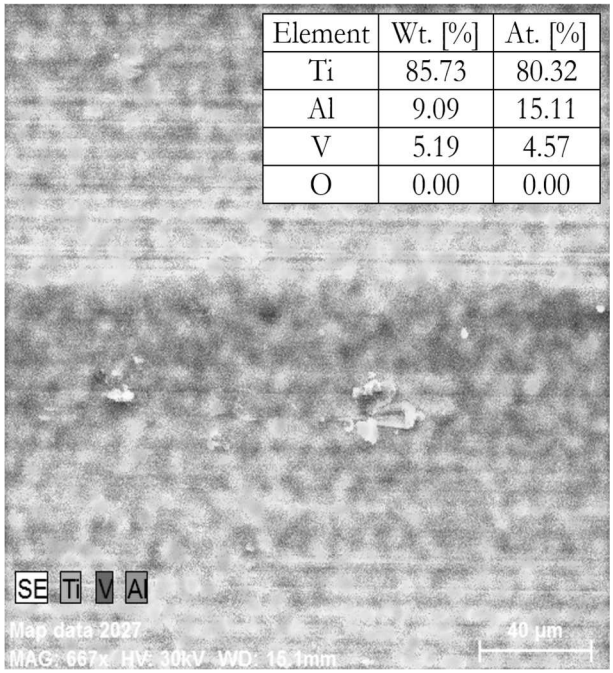

Element	Wt. [%]	At. [%]
Ti	85.73	80.32
Al	9.09	15.11
V	5.19	4.57
O	0.00	0.00

Fig. 32 *Result of EDS analysis and surface mapping*

As with the previous observation, the presence of oxide (O = 0.00 wt.%) was not documented on the surface of the experimental sample using EDS analysis and subsequent mapping (Fig. 32). In the following experimental sample labeled SR31, a microstructure was observed on the surface of the investigated material, with subsequent EDS analysis and mapping, which was documented in Fig. 33. On the surface of the examined material, we can observe NaCl particles that remained on the alloy after the corrosion load.

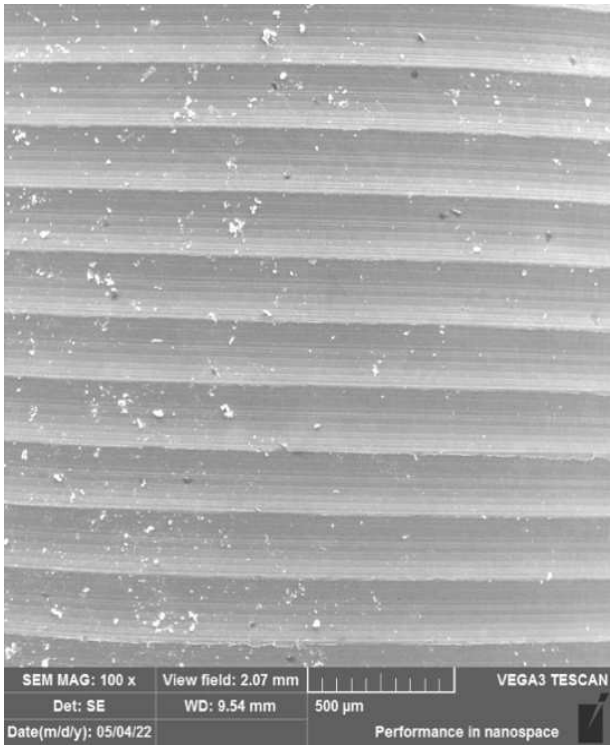

Fig. 33 *Surface condition of sample SR31*

indexed on http://www.webofscience.com and http://www.scopus.com

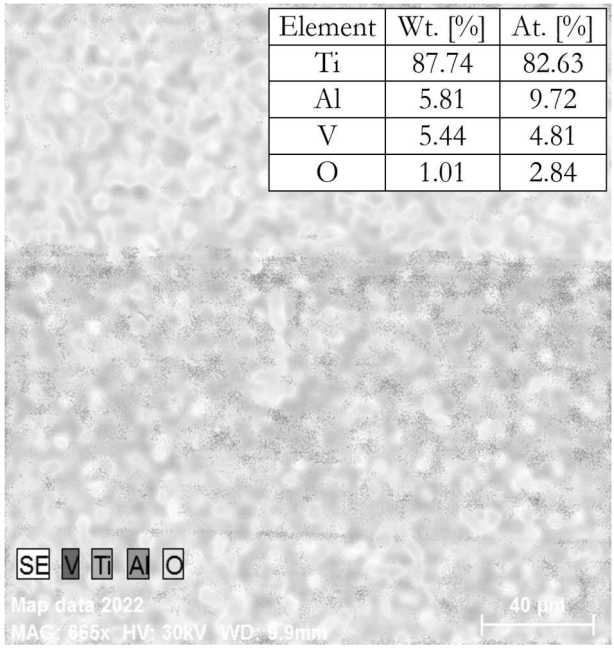

Fig. 34 *Result of EDS analysis and surface mapping*

In the observed experimental sample SR31, the occurrence of oxide on the surface of the examined material (O = 1.01 wt.%) was detected using EDS analysis. The unevenly distributed layer of oxide on the surface of the alloy was shown by surface mapping (Fig. 34).

In the next image (Fig. 35), we can observe the surface of an experimental sample made of titanium alloy Ti-6Al-4V. This sample was machined to a roughness parameter Ra of 0.3 and then subjected to corrosion loading in a salt chamber for 480 hours.

Fig. 35 *Surface condition of sample SR13*

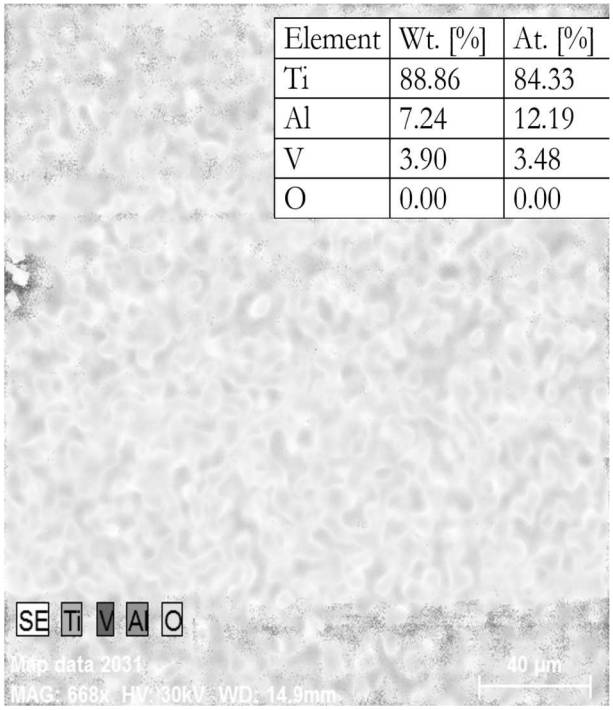

Fig. 36 *Result of EDS analysis and surface mapping*

In the observed sample labeled SR13, the presence of oxide on the surface of the material under investigation was not confirmed by EDS analysis (Fig. 36, O = 0.00 wt.%). There were traces of corrosion in the salt chamber on the surface of the investigated experimental sample.

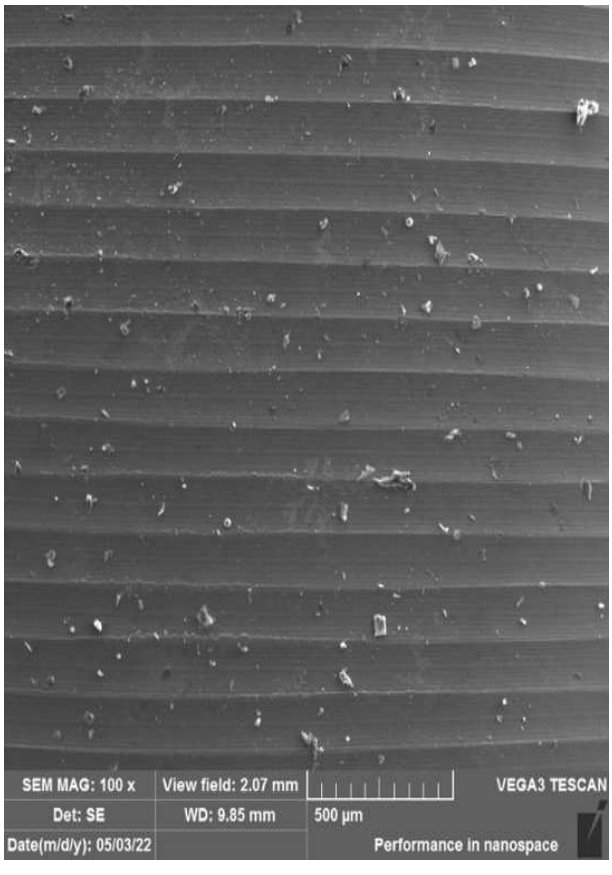

Fig. 37 *Surface condition of sample SR23*

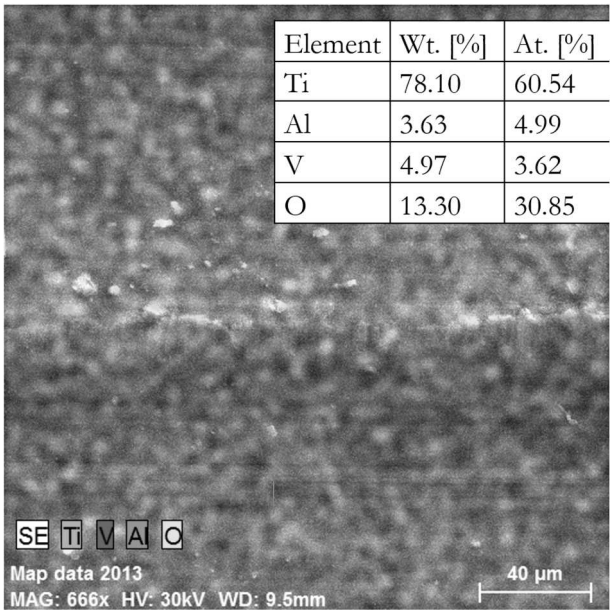

Fig. 38 *Result of EDS analysis and surface mapping*

On the next sample examined using EDS analysis, we can observe a large amount of oxide (O = 13.30 wt. %) on the surface of the experimental sample (Fig. 37). The EDS analysis was also confirmed by the subsequent mapping and area EDS analysis of the surface, where it can be observed that the oxide is unevenly distributed over the entire examined area (Fig. 38). The microstructure of the experimental sample was investigated in the following measurement of the investigated experimental sample marked SR33, which is machined to a roughness parameter of Ra 3.2 and subjected to corrosion loading in a salt chamber for 480 hours. Subsequently, an EDS analysis and mapping of the surface of the examined material was performed (Fig. 39, 40).

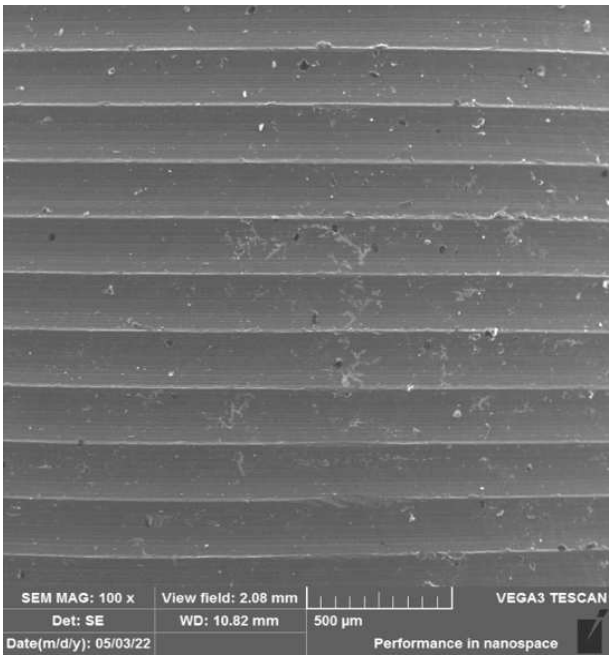

Fig. 39 *Surface condition of sample SR33*

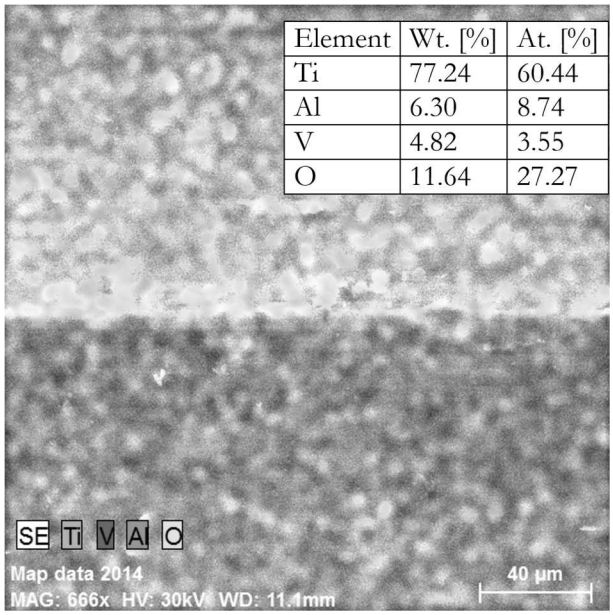

Fig. 40 *Result of EDS analysis and surface mapping*

In the experimental sample, using EDS analysis, there was a large amount of oxide (O = 11.64 wt.%) on the surface of the examined material. Subsequent mapping showed that the titanium oxide is distributed over the entire surface, the largest clusters of oxide are observable in the area of the grooves after machining.

The last observed sample that was subjected to corrosion stress in the salt chamber is SR34. The alloy was machined to a roughness parameter of Ra 3.2. Using an electron microscope, the microstructure of the surface was observed with subsequent EDS analysis and mapping, which is documented, see Fig. 41–42.

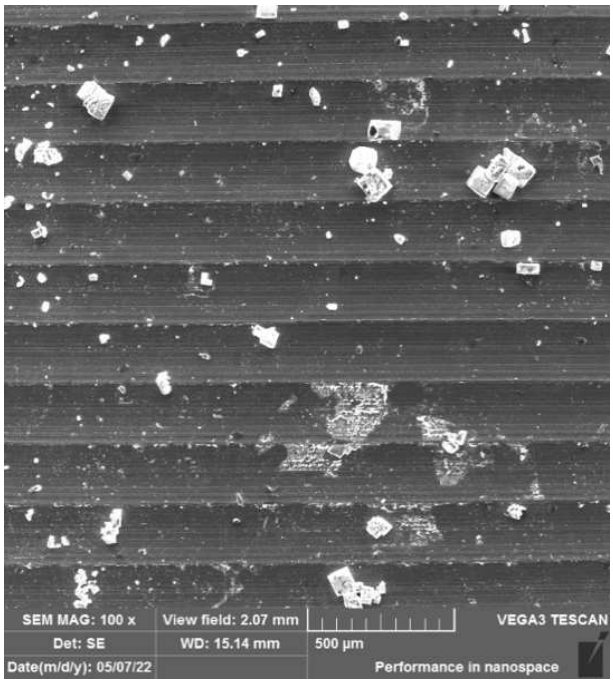

Fig. 41 *Surface condition of sample SR34*

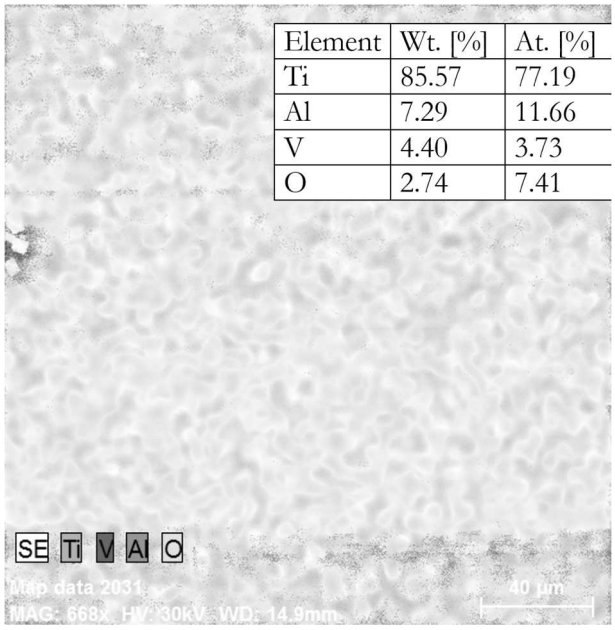

Fig. 42 *Result of EDS analysis and surface mapping*

In the case of the sample labeled SR34, a number of NaCl particles were observed on the surface of the material after the corrosion load in the salt chamber (Fig. 41). Using EDS analysis, titanium oxide was detected on the surface of the material. Subsequent mapping and surface EDS analysis (Fig. 42) confirmed the occurrence of oxide in the amount of O = 2.74 wt. %. Using mapping, a uniform and dense distribution of oxides over the entire surface of the experimental sample was also documented.

5.1 Layer rating

In the case of commercially pure titanium in the corrosion environment of the salt chamber, it was observed and measured that at all times of the corrosion load there was an increase in the oxidation layer of TiO_2 on the surface of the investigated experimental samples as the roughness parameter increased. For samples with the same roughness parameter, an increasing average thickness of the oxidation layer on the surface was observed with the time spent in the corrosion environment of the salt chamber, see Graph 1.

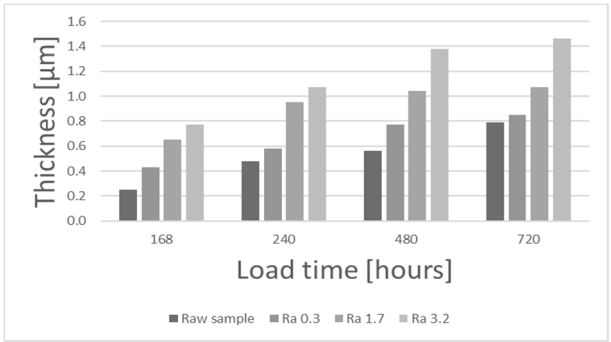

Graph 1 *Comparison of experimental samples of commercially pure titanium in a salt fog corrosion environment*

The amount of titanium oxide on the surface of the investigated experimental sample was measured and observed using EDS analysis and surface mass mapping on the titanium alloy Ti6Al4V, which was subjected to salt fog corrosion. This parameter was used to analyze the effect of roughness on the formation of a corrosion layer in a salt fog environment.

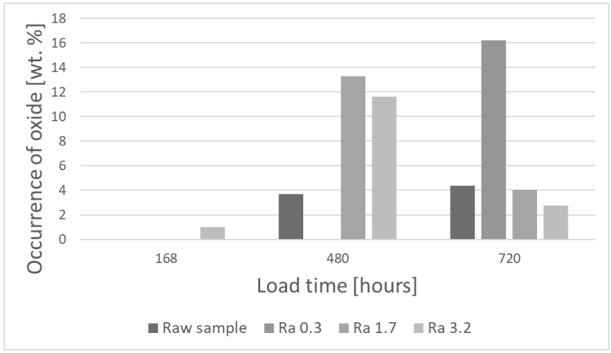

Graph 2 *Effect of roughness on the formation of a corrosion layer of experimental samples of the Ti-6Al-4V alloy in a corrosion environment of salt fog*

The same surface condition was observed for the samples that were subjected to salt spray corrosion loading for 240 hours as it was for 168 hours corrosion loading. For this reason, the graph does not show the values documenting these surfaces.

Under the corrosive load of salt fog for 168 hours, the occurrence of titanium oxide on the surface of the examined sample was measured using EDS analysis only in the sample labeled SR31, i.e. with a roughness parameter of 3.2. For all other roughness parameters, oxide was not measured at such a corrosion load time, Graph 2.

It was observed and subsequently documented on experimental samples subjected to corrosive medium salt fog for 480 hours that the presence of titanium oxide was measured on the surface of the untreated alloy using EDS analysis. At the smallest roughness parameter Ra 0.3, the appearance of oxide on the surface was not measured at the corrosion load of 480 hours as well as at 168 hours. At a roughness parameter Ra of 1.7, the largest occurrence of the oxidation layer was measured using EDS analysis. However, subsequent mapping showed that the experimental sample with a roughness parameter of Ra 3.2 had a more even and dense distribution of titanium oxide on the surface.

After the longest period of corrosion loading, 720 hours, the occurrence of oxide was measured and documented for the first time in a sample with a roughness parameter Ra of 0.3. In this experimental sample, EDS analysis was used to measure the largest mass amount of oxide of all the examined samples. However, both in the untreated sample and in the sample labeled SR14, an uneven occurrence of oxide

on the surface of the samples was observed and documented using surface EDS analysis and mapping. A sample with a roughness parameter of Ra 1.7 after 720 hours of corrosion loading has, using EDS analysis, the same as for samples after 480 hours of corrosion loading, a larger amount of titanium oxide on the surface than a sample with a roughness parameter of Ra 3.2. In both experimental samples, a uniform occurrence of oxide was observed using surface EDS analysis and surface mapping. A much denser distribution of titanium oxide was also observed for the sample with the largest roughness parameter Ra 3.2.

6 Conclusion

The experiment dealt with the effect of different roughness on the corrosion behavior of commercially pure titanium and titanium alloy Ti6Al4V in the corrosion environment of salt fog and physiological solution. Roughness parameters during machining of experimental samples were based on the article. The division of the experimental samples was therefore according to roughness into raw samples with a roughness parameter Ra of 0.3, 1.7 and 3.2. Subsequently, the samples were in a salt chamber at a temperature of 35 °C for 168, 240, 480 and 720 hours.

After sample preparation, samples of commercially pure titanium were evaluated on a VEGA Tescan 3 electron microscope, where the thickness of the TiO_2 oxidation layer was measured and observed at a magnification of 5000x. During the observation, 5 measurements were made, for which their arithmetic mean was subsequently calculated.

For all experimental samples of commercially pure titanium that were subjected to the corrosion load of salt fog, it can be observed that with increasing roughness, the average TiO_2 oxidation layer grows on the surface of the investigated material. It can be seen from Graph 1 that the average thickness of the oxidation layer increases not only with increasing roughness parameters, but also with increasing time for the same roughness parameters. From these measurements, it was found that the roughness parameter has an effect on the corrosion behavior of commercially pure titanium in the corrosion environment of salt fog.

In the case of the Ti6Al4V titanium alloy, after measuring and evaluating the results after corrosion loading in salt fog, it can be stated that the roughness parameter has an effect on the mass percentage of titanium oxide on the surface of the examined samples at corrosion loading times of 168 and 420 hours. No longer for samples exposed to corrosion for 720 hours. However, the roughness parameter has an effect on a more even and dense distribution of the oxide on the surface.

For further possible experiments on the corrosion behavior of titanium and its alloys, it would be necessary to conduct an experiment in the corrosion environment of physiological solution, whether the combination of a longer time and the same roughness will have an effect on the formation of a more stable oxidation layer of TiO_2 on the surface. Alternatively, to monitor whether the increasing corrosion load time of experimental samples of titanium alloy Ti6Al4V in salt mist or physiological solution, due to the formation of a more stable surface oxidation layer, will be beneficial or not.

Acknowledgement

This publication is the result of support under the SGS of UJEP-SGS-2021-48-002-3.

References:

[1] KREJČÍ, S. Protikorozní ochrana kovových konstrukcí a strojírenských zařízení organickými povlaky, anorganickými nekovovými povlaky a kovovými povlaky. Brno: *TESYDO, 2017*. ISBN isbn978-80-87102-18-3.

[2] HLUCHÝ, M., HANĚK, V. *Strojírenská technologie 2*. 2., upr. vyd. Praha: Scientia, 2001. ISBN isbn80-7183-245-6

[3] KRAUS, V. *Povrchy a jejich úpravy*. Plzeň: Západočeská univerzita, 2000. ISBN isbn978-80-7082-668-3

[4] SCHUTZ, R.W. Utilizing titanium to successfully handle chloride process environments. *CIM Bull.* 2002; 95: 84-88

[5] Titanium and titanium alloys: fundamentals and applications. Editor Christoph LEYENS, editor PETERS, *M. Weinheim: Wiley-VCH*, 2003. ISBN isbn3-527-30534-3

[6] YU, S., Corrosion Resistance of Titanium Alloys, Corrosion: Fundamentals, Testing, and Protection, Vol 13A, ASM Handbook, ASM International, 2003, p 703–711 in *ASM handbook*. 10th editon. Materials Park, Ohio: ASM International, [1990]-<[2016]>. ISBN isbn0-87170-705-5

[7] SHOESMITH, D. Corrosion of Titanium and Its Alloys, Reference Module in Materials Science and Materials Engineering. *Elseiver Inc*, 2018

[8] ROUDNICKA M, MISURAK M, VOJTECH D. Differences in the Response of Additively Manufactured Titanium Alloy to Heat Treatment - Comparison between SLM and

EBM. *Manufacturing Technology*. 2019;19(4):668-673

[9] DELIGIANNI, D. D., KATSALA, N., LADAS, S., SOTIROPOULOU, D., AMEDEE, J., MISSIRLIS, Y. F. Effect of surface roughness of the titanium alloy Ti-6Al-4V on human bone marrow cell response and on protein adsorption, *Biomaterials 22* (2001) 1241 – 1251

[10] HREN I, KUŚMIERCZAK S, HORKÝ R, MACH J. Analysis of the Effect of Heat Treatment and Corrosion Load on the Microstructure and Microhardness of the Ti6Al4V Alloy. *Manufacturing Technology*. 2022;22(4):414-422

[11] HE, G., HAGIWARA, M. Ti alloy design strategy for biomedical applications, Volume 26, Issue 1, January 2006, Pages 14-19

[12] MÁDL, J. Integrita obrobených povrchů z hlediska funkčních vlastností. Ústí nad Labem: FVTM UJEP, 2008. *Knižnice strojírenské technologie*. ISBN 978-80-7414-095-2

[13] NOVÁK, M. Broušení kovů. Ústí nad Labem: Univerzita J.E. Purkyně v Ústí nad Labem, 2019. ISBN 978-80-7561-174-1

[14] TEICHMANOVA A, MICHALCOVA A, NECAS D. Microstructure and Phase Composition of Thin Protective Layers of Titanium Aluminides Prepared by Self-propagating High-temperature Synthesis (SHS) for Ti-6Al-4V Alloy. *Manufacturing Technology*. 2022;22(5):605-609

[15] KLETEČKA, J., a FOŘT, P. Technické kreslení. 2., opr. vyd. Brno: Computer Press, 2007. Učebnice (Computer Press). ISBN isbn978-80-251-1887-0

[16] FEKRY, A. M., TAMMAM, R.H. The Influence of Different Anions on the Corrosion Resistance of Ti-6Al-4V Alloy in Simulated Acid Rainwater, February 2014 Industrial & Engineering Chemistry Research 53(8): Pages 2911–2916

[17] TANG, J., LUO, H.Y., ZHANG, Y.B. Enhancing the surface integrity and corrosion resistance of Ti-6Al-4V titanium alloy through cryogenic burnishing, *Int J Adv Manuf Technol* (2017) 88: Pages 2785–2793

[18] DONACHIE, M. J. Titanium: a technical guide. 2nd ed. *Materials Park: ASM International*, 2004, vii, 381 s. ISBN 08-717-0686-5

[19] RMI TITANIUM COMPANY. Titanium alloy guide. 2000

[20] FOUSOVA M, VOJTECH D. Influence of Process Conditions on Additive Manufacture of Ti6Al4V Alloy by SLM Technology. *Manufacturing Technology*. 2017;17(5):696-701

[21] LATTNER R, HOLEŠOVSKÝ F, NOVÁK M, VRABEĽ M. Grinding of Titanium Alloy Ti6Al4V with Silicon Carbide Grinding Wheel. *Manufacturing Technology*. 2016;16(1):159-162

[22] DEARNLEY, P.A, DAHMA, K.L., ÇIMENOGLU, H. The corrosion–wear behaviour of thermally oxidised CP-Ti and Ti–6Al–4V, *Wear 256* (2004), Pages 469–479

[23] THOMPSON, D.H. General Tests and Principles. Handbook on Corrosion Testing and Evaluation, John Wiley and Son Inc., New York, 1971

[24] ČSN ISO 8407: Koroze kovů a slitin, Odstraňování korozních zplodin ze vzorků podrobených korozním zkouškám. Leden 1995. Praha: Český normalizační institut, 1995,12 s

[25] ČSN 03 8137: Ochrana proti korozi, KOVY, SLITINY A KOVOVÉ POVLAKY: Metalografické vyhodnocování korozního napadení, Praha: Český normalizační institut, 1990, 20 s

[26] NOVÁK, P. a kol., Korozní inženýrství, verze 1.02 CD, ÚKMKI VŠCHT Praha 2002, 63 s

[27] ČSN EN ISO 12944-2: Nátěrové hmoty – Protikorozní ochrany ocelových konstrukcí ochrannými nátěrovými systémy – Část 2: Klasifikace vnějšího prostředí

[28] KOCICH, J., a TULEJA, S. Korozia a ochrana kovov. 4. vyd. Košice, 1998. ISBN 80-7099-393-6

[29] Microstructure and properties of materials [online]. Singapore: World Scientific, 2000, 436 s. [cit. 2012-01-23]. ISBN 981-02-4180-1

[30] ČSN 03 8212: Zabezpečování jakosti korozních zkoušek v umělých atmosférách. Praha: Český normalizační institut, 1994

[31] ŠIMŮNEK, A. a kol. Dentální implantologie, druhé přepracované a doplněné vydání. Hradec Králové: Nucleus, 2008, 290 s. ISBN 978-80-87009-30-7

[32] PTAČEK, L. et al. Nauka o materiálu II.Brno: CERN, s.r.o., 2002. 395 s. ISBN 80-7204-248-3

[33] ASKELAND, D. R., PHULÉ, P. P. Science and engineering of materials.5th ed. Toronto: Thomson, 2006, 863 s. ISBN 0-534-55396-6

[34] BODUNRIN, M. O., CHOWN, L. H., VAN DER MERWE, J.W., ALANEME, K.K., OGANBULE CH., KLENAM, D.E.P., MPHASHA, N.P. Corrosion behavior of titanium alloys in acidic and saline media: role of alloy design, passivation integrity, and electrolyte modification

[35] GUDIĆ, S., VRSALOVIĆ, L., KVRGIĆ, D. NAGODE, A. Electrochemical Behaviour of Ti and Ti-6Al-4V Alloy in Phosphate Buffered Saline Solution, *Materials 2021*, Pages 14, 7495

[36] JUNFEI, O., MINGZHI, L., WEN, L., FAJUN, W., MINGSHAN, X., CHANGQUAN, L., Corrosion behavior of superhydrophobic surfaces of Ti alloys in NaCl solutions, March 2012, Applied Surface Science 258(10):4724-4728

[37] POHRELYUK, I. M., FEDIRKO, V. M., TKACHUK, O. V., PROSKURNYAK, R. V., Corrosion resistance of Ti–6Al–4V alloy with nitride coatings in Ringer's solution, *JOM,* Volume 63, Issue 6, pages 35-40